Moving source depth estimation based on Green's function retrieval with a vector sensor

Zhuang Cheng, Yanqun Wu, Zhengliang Hu, Jun Wang and Yongming Hu

Academy of Ocean Science and Engineering
National University of Defense Technology
Changsha, China
Email: wuyanqun@nudt.edu.cn

***Abstract*—Underwater acoustic source localization has attracted wide interests, and the source depth estimation is more difficult than that of source range and bearing. The performance of Matched Field Processing (MFP) degrades greatly under environment parameter mismatches, which makes it limited in practice. Varieties of robust methods have been proposed to relieve the mismatch problems. T. C. Yang proposed a depth estimation for a moving CW source with a single pressure sensor [1], by which little information is required. This paper extends this method to a single vector sensor. This paper starts from the particle velocity expressions in normal-mode method to derive Green's functions for horizontal and vertical particle velocity respectively, and theoretically analyze the characteristics of the Green's functions, then give proper objective functions to estimate the source depth. Numerical simulations validate the proposed method, and show that joint signal processing of the pressure and the vertical particle velocity improves the performance under inexact SSP.**

***Index Terms*—Depth estimation, data-driven, Green's function retrieval, moving source, vector sensor.**

I. Introduction

The estimation of source depth in underwater acoustic waveguide is more difficult than that of source range and bearing. Matched field processing (MFP) takes advantage of multipath effect by matching received data with the replica field calculated by acoustic propagation modal at a candidate source location [2]. However, its performance heavily relies on how accurately we understand and sample the environment, and degrades under environmental mismatch. To solve this problem, a variety of solutions were proposed, known as mismatch tolerant MFP methods, e.g. multiple neighboring location constraints MFP [3], Bayesian MFP [4]. Other solutions called data-driven/data-based MFP methods estimate environment parameters or mode depth function from received data [5].

A range-independent waveguide can be characterized by the depth-dependent Green's function, which allows a class of methods called modal inverse techniques to inverse the geoacoustic parameters from the depth-dependent Green's function [6]. Similar methods can estimate the source depth. Hankel transformation or its asymptotic expression of sound field over enough range span will give an estimation of depth-dependent Green's function. The characteristic of this method is that, only one receiver at least is all we need to estimate the depth of a moving source, while for a static source, horizontal array of certain aperture is needed. In other words, sound field sample of a certain range span is necessary.

A vector sensor consists of a pressure sensor and two or three orthogonally oriented velocity sensor, and samples the acoustic pressure and the particle velocity simultaneously. Although connected by Euler's equation, neither particle velocity nor pressure could characterize the acoustic field by itself. One main advantage of a vector sensor over a traditional scalar sensor is that it allows varieties of joint signal processing approaches by taking use of more available acoustic information.

In this paper, we present a model-independent approach to source depth estimation using only one sensor, and extend it to the application of a vector sensor. Theoretical analysis and simulations show that both the pressure field and the vertical velocity field give reasonable source depth estimation and joint signal processing improves the performance of depth estimation under inexact SSP. This article is organized as follows. In Section II, we introduce a depth estimation method with a scalar pressure sensor, and derive Green's function of horizontal and vertical velocities, then give proper objective functions for depth estimation. In Section III, we apply this approach to numerical simulations with the same environment as that in SWellEx96 experiment, except that we use a vector sensor here. Section IV summarizes the paper.

II. Formulation of Depth Estimation Problem

A. Review of the depth estimation method with a scalar pressure sensor

We consider a horizontally stratified and range-independent ocean model. The field $p(r, z_r)$ due to a point source of frequency ω at range $r = 0$ and depth $z = z_s$ can be expressed as the zero-order Hankel transform of the depth-dependent Green's function $G(k_r, z_r)$ and vice versa,

$$p\left(r, z_r\right) = \int_0^\infty G\left(k_r, z_r\right) J_0\left(k_r r\right) k_r dk_r \tag{1}$$

$$G\left(k_r, z_r\right) = \int_0^\infty p\left(r, z_r\right) J_0\left(k_r r\right) r dr \tag{2}$$

where r is the horizontal range; k_r is the horizontal wavenumber; and J_0 is the zero-order Bessel function.

978-1-5386-3142-3/17/$31.00 ©2017 IEEE

Using the asymptotic form of the Bessel function in Eqs. 1 and 2, it gives

$$p(r,z_r) \sim \frac{e^{-i\pi/4}}{\sqrt{2\pi r}} \int_0^\infty G(k_r,z_r)\, e^{ik_r r}\sqrt{k_r}\,dk_r \qquad (3)$$

$$G(k_r,z_r) \sim \sqrt{\frac{2\pi}{k_r}} e^{i\pi/4} \int_0^\infty p(r,z_r)\, e^{-ik_r r}\sqrt{r}\,dr \qquad (4)$$

where $k_r > 0$, $r > 0$ and $k_r r \gg 1$.

In a range-independent environment, the pressure can expressed as a sum of normal modes

$$p(r,z_r) = \frac{i}{4\rho(z_s)} \sum_{n=1}^{N} \phi_n(z_s)\,\phi_n(z_r)\, H_0^{(1)}(k_n r) \qquad (5)$$

where ϕ_n is the mode-depth function, $H_0^{(1)}$ is the zero-order Hankel function of the first kind, k_n is the modal horizontal wavenumber.

By the asymptotic form of the Hankel function, we have

$$p(r,z_r) \sim \frac{i}{\rho(z_s)\sqrt{8\pi}} e^{-i\pi/4} \sum_{n=1}^{N} \phi_n(z_s)\,\phi_n(z_r)\, \frac{e^{ik_n r}}{\sqrt{k_n r}} \qquad (6)$$

Taking it into Eq. 4 and integrating over a finite aperture R, it gives

$$G_p(k_r,z_r) \sim \frac{-1}{2\rho(z_s)} \sum_{n=1}^{N} \phi_n(z_s)\,\phi_n(z_r) \frac{1}{\sqrt{k_r k_n}} \left(\frac{e^{-i(k_r-k_n)R}-1}{k_r-k_n} \right) \qquad (7)$$

It can be seen that Green's function has first order poles at horizontal wavenumbers corresponded to the modal eigenvalues $k_r = k_n$, leading to peaks of finite height and width in its Green's function. One can estimate the source depth with peak values of Green's function through a proper objective function. Yang gives a choice in [1],

$$D_p(z) = \left| \sum_{n=1}^{N} \phi_n(z)\, \frac{G_p(k_n,z_r)}{\bar{\phi}_n(z_r)} \right|^2 \qquad (8)$$

where $\bar{\phi}_n(z_r)$ is a regularized mode depth function given by $\bar{\phi}_n^{-1}(z_r) = \phi_n(z_r) / \left[\phi_n^2(z_r) + \Delta^2\right]$ where Δ is chosen to prevent blow up of the inverse mode depth function at zero-crossing points. The mode depth function here to use will be calculated with a nominal SSP, which is good enough for coarse estimation of the source depth [1]. The normal modes calculated by nominal SSP will be matched up with the peak values picked from Green's function according to horizontal wavenumbers with a certain tolerance.

B. Green's functions and objective functions for the particle velocity sensors

The horizontal and vertical particle velocity components v_r and v_z are related to the pressure by Euler's Equation. Incorporating Eq. 6 to Euler's Equation gives

$$v_r(r,z_r) = \frac{-i}{\rho^2\omega\sqrt{8\pi}} e^{-i\pi/4} \sum_{n=1}^{N} \phi_n(z_s)\,\phi_n(z_r) \sqrt{\frac{k_n}{r}} e^{ik_n r} \qquad (9)$$

$$v_z(r,z_r) = \frac{-1}{\rho^2\omega\sqrt{8\pi}} e^{-i\pi/4} \sum_{n=1}^{N} \phi_n(z_s)\,\phi_n'(z_r) \sqrt{\frac{1}{k_n r}} e^{ik_n r} \qquad (10)$$

where $\phi_n'(z_r) = (\partial/\partial z_r)\,\phi_n(z_r)$ is the derivative of the mode depth function with respect to z_r.

Taking Eqs. 9 and 10 into Eq. 4 and integrating over a finite range aperture R respectively, we have the Green's functions for v_r and v_z in the far field

$$G_{v_r}(k_r,z_r) \sim \frac{i}{2\rho^2\omega} \sum_{n=1}^{N} \phi_n(z_s)\,\phi_n(z_r) \sqrt{\frac{k_n}{k_r}} \left(\frac{e^{-i(k_r-k_n)R}-1}{k_r-k_n} \right) \qquad (11)$$

$$G_{v_z}(k_r,z_r) \sim \frac{i}{2\rho^2\omega} \sum_{n=1}^{N} \phi_n(z_s)\,\phi_n'(z_r) \sqrt{\frac{1}{k_n k_r}} \left(\frac{e^{-i(k_r-k_n)R}-1}{k_r-k_n} \right) \qquad (12)$$

For v_r, we choose the same objective function as Eq. 8, while for v_z the objective function is modified to

$$D_{v_z}(z) = \left| \sum_{n=1}^{N} \phi_n(z)\, \frac{G_{v_z}(k_n,z_r)}{\bar{\phi}_n'(z_r)} \right|^2 \qquad (13)$$

For convenient discussion, we introduce two definitions by analogy with in beamforming method called the width of main lobe and the side lobe level to describe the performance of depth estimation.

III. Numerical Simulation and Discussion

In this paper, we consider a range-independent waveguide with the same parameters of the SWellEx96 expriment which was conducted in May 1996, west of Point Loma in San Diego, CA [7], as seen from Fig. 1. A vector sensor is deployed at a depth of 200 m, and recorded at a sample rate of 500 Hz. A CW source of 40 Hz is towed at a constant velocity of 2.5 m/s, starting from a range of 1000 m to 7750 m. The acoustic field $X(r(t), z_r)$ is generated by the KRAKEN normal-mode program, where X donate the pressure field p and particle velocity field v_r or v_z, and the recorded signal is generated with

$$x(r(t), z_r, t) = X(r(t), z_r) \times e^{i2\pi f t} \qquad (14)$$

The simulation signal is divided into blocks, each with 1000 samples, corresponding to a range interval of 5 m, which is enough for Green's function retrival according to the Nyquist's sampling theorem. Then the acoustic field is estimated for each block of data, one could reach more details in [1]. Green's function of pressure field could be retrieved with the pressure field and Eq. 4. Same transformation will be applied for horzontal and vertical velocity.

Figure 2 shows the comparison of Green's function retrievals of pressure, horizontal and vertical particle velocity. We can see that high-order modes contribute more to vertical velocity because they have higher grazing angles. Similarly,

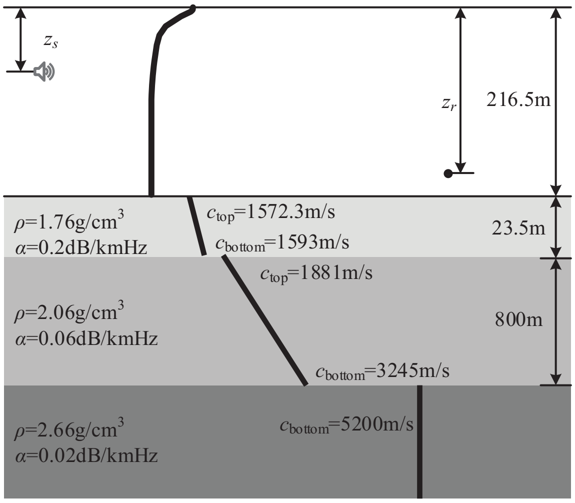

Fig. 1: Schematic of shallow water waveguide in SWellEx96 experiment.

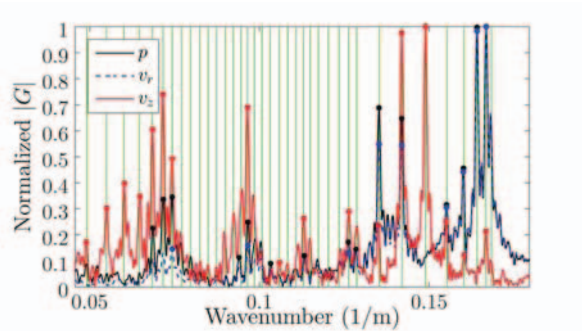

Fig. 2: Comparison of normalized Green's function retrievals of p, v_r and v_z, point markers of corresponding color indicate the peaks picked by a peak picking program. Vertical green lines indicate the wavenumbers of all the excited normal modes in this simulation.

low-order modes contributes more to pressure and horizontal velocity because of their lower grazing angles. Meanwhile, prominent peaks of G_p and G_{v_z} show a kind of complementarity because of the different fluctuating behavior between $\phi_n'(z_r)$ and $\phi_n(z_r)$. G_{v_r} is analogous to G_p since they share the same items $\phi_n(z_s)\phi_n(z_r)$, which determine the excitation amplitude of n-order mode. Since G_{v_r} provides no more information than G_p, we'll concentrate on comparisons between G_p and G_{v_z} in the simulations below.

Consider a situation of depth estimation with only one peak value of Green's function for convenient dicussion. From Eqs. 8 and 13, it's found that the oscillation of depth estimation $D(z)$ is determined by the period of the mode depth function. In other words, the higher-order modes we used, the narrower main lobe of depth estimation we obtained.

Figure 3 shows a comparison of depth estimation with peaks corresponding to different orders of modes. Figures 3a shows the first 5 peaks of G_p and G_{v_z} picked by a program, and

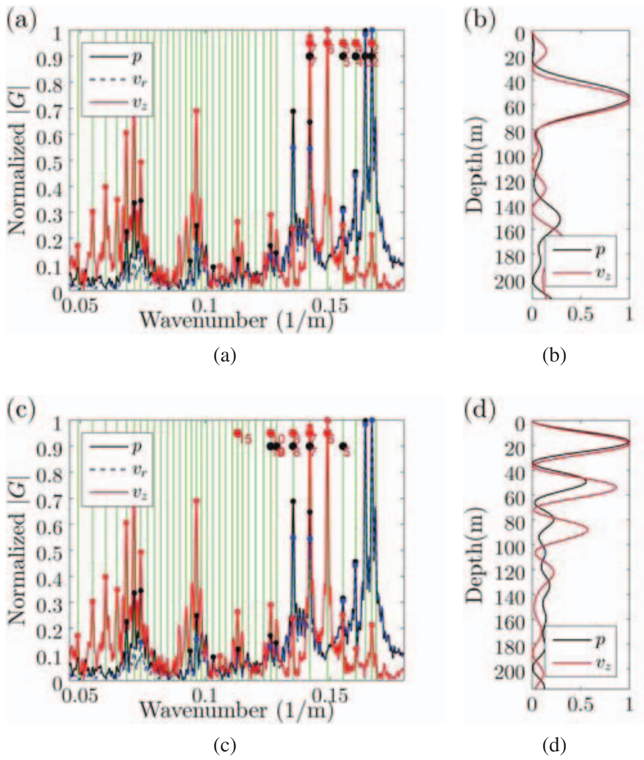

Fig. 3: Comparisons of depth estimation with different modes by p and v_z. Point markers in corresponding color in (a) and (c) shows the 5 modes selected to estimate the source depth. (b) and (d) are the source depth estimations.

3c shows the 4th to 8th peaks of G_p and G_{v_z}. Figures 3b and 3d are the corresponding estimations. We can draw a conclusion that peaks of low-order modes will reduce the side lobe of depth estimation, while peaks of higher-order modes will narrow the width of main lobe.

Spontaneously, one would wonder if it is feasible to take more peaks as much as possible into account to obtain a robust estimation with a narrow main lobe. For the complementarity between G_p and G_{v_z}, we use them for joint signal processing, and give a modified objective function as

$$D_{pv_z}(z) = \left| \sum_{n \in N_p} \phi_n(z) \frac{G_p(k_n, z_r)}{\bar{\phi}_n(z_r)} + A \sum_{m \in M_{v_z}} \phi_m(z) \frac{G_{v_z}(k_m, z_r)}{\bar{\phi}'_m(z_r)} \right|^2 \tag{15}$$

where N_p and M_{v_z} is the mode sets picked by a peak picking program from G_p and G_{v_z} respectively, and $A = \sqrt{\max(D_p)/\max(D_{v_z})}$ is a factor to normalize the second item in the right side of Eq. 15 to be comparable to the first item.

Figure 4 shows the comparison of depth estimation with the p-only, the v_z-only and the joint methods. Since more peaks of high-order modes are retrieved from Green's function

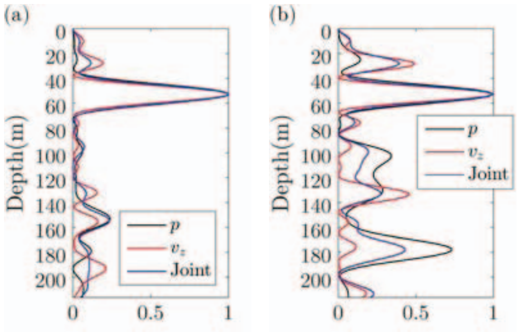

(a) (b)

Fig. 4: Comparison of depth estimation with p, v_z and $p - v_z$ joint signal processing. (a) is the depth estimation with all peaks picked, (b) uses a isovelocity nominal SSP of 1500 m/s.

of vertical velocity, processing of G_{v_z} and joint processing give depth estimations with narrower main lobes. Joint signal processing take advantages of more orders of modes and give ambiguity functions with lower side lobe under SSP mismatch.

IV. Conclusion

The depth-dependent Green's function contains enough information to estimate source depth, and can be estimated by taking Hankel transform to the pressure/particle velocity field of a certain range span. Taking account of Green's function's peaks corresponding to higher-order modes gives a depth estimation with a narrower main lobe. Numerical simulations show that Green's function of the vertical particle velocity field gives a depth ambiguity function with narrower main lobe, since the vertical velocity is mainly excited by high-order modes. Joint signal processing of the pressure and the vertical particle velocity gives more robust depth estimations than the pressure only method under inexact SSP.

Acknowledgment

This work is supported by National University of Defense Technology under Grants No. ZK16-03-31.

References

[1] T. Yang, "Source depth estimation based on synthetic aperture beamfoming for a moving source," *The Journal of the Acoustical Society of America*, vol. 138, no. 3, pp. 1678–1686, 2015.

[2] A. Tolstoy, *Matched field processing for underwater acoustics*. World Scientific, 1993.

[3] H. Schmidt, A. Baggeroer, W. Kuperman, and E. Scheer, "Environmentally tolerant beamforming for high-resolution matched field processing: Deterministic mismatch," *The Journal of the Acoustical Society of America*, vol. 88, no. 4, pp. 1851–1862, 1990.

[4] A. Richardson and L. Nolte, "A posteriori probability source localization in an uncertain sound speed, deep ocean environment," *The Journal of the Acoustical Society of America*, vol. 89, no. 5, pp. 2280–2284, 1991.

[5] M. D. Collins and W. Kuperman, "Focalization: Environmental focusing and source localization," *The Journal of the Acoustical Society of America*, vol. 90, no. 3, pp. 1410–1422, 1991.

[6] S. Rajan, G. V. Frisk, K. M. Becker, J. F. Lynch, G. Potty, and J. Miller, "Modal inverse techniques for inferring geoacoustic properties in shallow water," *Important Elements in: Geoacoustic Inversion, Signal Processing, and Reverberation in Underwater Acoustics*, vol. 2, pp. 165–234, 2008.

[7] Information and data for the SWellEx96 experiment available at http://swellex96.ucsd.edu/index.htm.